COMSOL Multiphysics Modeling of a 20-W Microwave Electrothermal Thruster

Enyu Gao* and Sven G. Bilén†
Department of Electrical Engineering, The Pennsylvania State University, University Park, PA
*Enyu Gao, 304 Electrical Engineering East, University Park, PA 16802, eug11@psu.edu
†Sven G. Bilén, 213N Hammond, University Park, PA 16802, sbilen@ psu.edu

Abstract: The Microwave Electrothermal Thruster (MET) is a space electric propulsion device that uses an electromagnetic resonant cavity within which a free-floating plasma is ignited and sustained, heating a propellant gas that is that exhausted out of a gas-dynamic nozzle. For an empty cavity without any perturbing regions—e.g., dielectric regions or antenna regions—it is fairly straightforward to accurately calculate the cavity's resonant frequency and describe the electric field intensity distribution within the cavity. However, actual METs do contain perturbing regions, which means that analytical solutions are no longer possible to fully characterize the device. Hence, we have employed numerical simulations using COMSOL Multiphysics to simulate the electric field intensity and distribution within the MET's resonant cavity.

Keywords: microwave, resonant cavity, numerical modeling, electric propulsion

1. Introduction

The Microwave Electrothermal Thruster (MET) is an electric propulsion device that uses an electromagnetic resonant cavity within which free-floating plasma is ignited and sustained in a propellant gas.[1] The propellant heated by the plasma is accelerated through a gas dynamic nozzle and exhausted to generate thrust. The microwave thruster is similar to a conventional arcjet in as much as they both use electrical energy to generate high temperature plasmas that, in turn, heat a flowing gas propellant followed by a nozzle expansion to obtain thrust. However, the MET is characterized by a free floating arc plasma discharge, while an arcjet utilizes an arc discharge formed between two electrodes to heat a propellant gas. The main difference is that the MET plasma is free-floating and, thus, the system does not suffer from the lifetime-limiting electrode erosion problems that are characteristic of the arcjet. The MET potentially offers thrust and specific impulse comparable to arcjets with higher efficiency at low power levels and longer lifetimes. The location of the discharge, which forms at the region of maximum microwave power density, is determined by the pattern of electric power density within a microwave resonant cavity absorption chamber. Proper cavity design produces patterns that result in an axially located plasma that is positioned directly upstream from a nozzle incorporated into one end of the cavity. Therefore, while some nozzle erosion may be a concern, erosion is not of a critical electrical component as is the case with the conventional arcjet.[2]

The MET's resonant cavity operates in the transverse magnetic TM^{z}_{011} mode, which is optimal for producing an axial, free-floating plasma. The resonant cavity also serves as the pressurized chamber within which cold propellant gas is heated to a high temperature followed by a gas dynamic expansion through a converging–diverging nozzle to obtain a high velocity exhaust. Hence, there are a number of coupled physical processes that must be captured, including electromagnetic cavity modes, gas dynamics, gas breakdown physics, and heat flow.

With respect to electromagnetic modeling of MET cavities, a number of groups have explored various methods for injecting microwave energy into the gas. Early work examined the electric field structure in a cavity with a heating chamber placed axially down the center.[3,4,5] This led to a design wherein the plasma created in the center column provided a somewhat perturbed coaxial-like geometry for the fields. Subsequent work[6,7,8] led to abandoning the central heating chamber and allowing the plasma to be free floating, which is the present configuration of the MET. It is interesting to note that some recent work has explored the coaxial configuration once again as a method for providing intense electric fields at the nozzle.[9]

This paper begins with a discussion of the MET as well as the theory of its operation, including parameters that help determine field strength and resonant frequency. Numerical electromagnetic simulations of several cavity electromagnetic fields are described and results presented.

2. MET Principles of Operation

The MET, shown schematically in Fig. 1, consists of a circular cross-section resonant cavity operating in the TM^z_{011} mode. This resonant mode, shown in Fig. 2 for an empty cavity, is characterized by regions of high electric energy density on the cavity axis at the endplates, and in the annular region circumscribing the cavity midplane. Properly selecting the height-to-diameter ratio of the cavity causes the electric energy density at the endplates to be much greater than at the midplane. The resonant cavity is a circular cross-section waveguide shorted by two conducting endplates. One endplate contains a nozzle and the other contains an antenna for inputting microwave power, each along the cavity's axis.

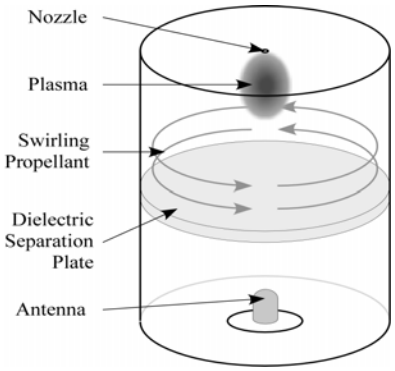

Figure 1. MET schematic

The MET's resonant cavity operates in the transverse magnetic TM^z_{011} mode, which is optimal for producing an axial, free-floating plasma at one end of the cavity. In this mode, the electric field strength is high at the cavity's ends. Proper selection of the cavity's height-to-diameter ratio causes the electric field strength at the end plates to be much greater than at the midplane of the cavity. The free-floating ac plasma discharge forms at regions of maximum power density, i.e., an axially located plasma that is positioned directly upstream from a nozzle incorporated into one end of the cavity.

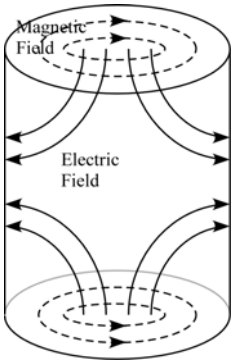

Figure 2. TM^z_{011} electromagnetic mode

2.1 Resonant Cavity Theory at TM^z_{011} mode

The electromagnetic field theory of the MET begins with Maxwell's Equations, from which we can develop second-order differential equations with wave solutions. Solutions of the wave equations can be found in the form of vector potentials. The MET resonant cavity is of cylindrical shape, so it is natural to use cylindrical coordinates for theoretical analysis. The resonant cavity is assumed to be a perfect conductor filled with a homogeneous, lossless, source-free medium. For such a cavity, it can be shown that the electric and magnetic field components and the resonant frequency for the TM^z_{011} resonant mode are given by[10]

$$E_r = j\frac{B_{011}}{\omega\mu\varepsilon}\frac{\chi_{01}}{a}\frac{\pi}{h}J_0'\left(\chi_{01}r/a\right)\sin\left(\pi z/h\right) \quad (1)$$

$$E_\phi = 0 \quad (2)$$

$$E_z = -j\frac{B_{011}}{\omega\mu\varepsilon}\left(\frac{\chi_{01}}{a}\right)^2 J_0\left(\chi_{01}r/a\right)\cos\left(\pi z/h\right) \quad (3)$$

$$H_r = 0 \quad (4)$$

$$H_\phi = -\frac{B_{011}}{\mu}\frac{\chi_{01}}{a}J_0'\left(\chi_{01}r/a\right)\cos\left(\pi z/h\right) \quad (5)$$

$$H_z = 0 \quad (6)$$

$$\left(f_{\text{res}}\right)^{\text{TM}^z}_{011} = \frac{1}{2\pi\sqrt{\mu\varepsilon}}\sqrt{\left(\chi_{01}/a\right)^2 + \left(\pi/h\right)^2} \quad (7)$$

Fig. 3 shows the TM^z_{011} resonant frequency for an empty cavity, with $\mu = \mu_0$ and $\varepsilon = \varepsilon_0$, as a function of h/a for different cavity radii. The effect of varying cavity geometry can be seen. As the cavity height and radius are increased, the resonant frequency decreases. Similarly, perturbations inside the cavity, such as the presence of dielectric inserts or plasma, can alter the resonant frequency causing its accurate analytical prediction to be difficult.

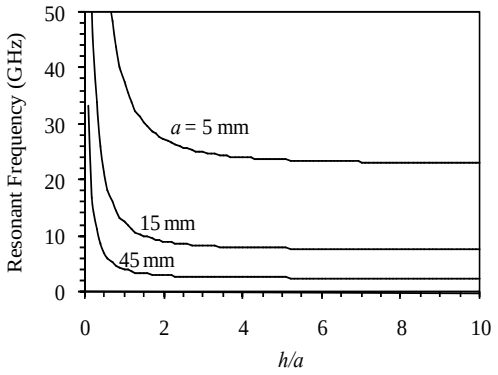

Figure 3. Resonant frequency variation with *h/a.*

For a given desired resonant frequency, there exist an infinite number of combinations of cavity height and radius that satisfy Eqn. 7. The TM^z_{011} resonant mode has regions of high electric field strength on the axis near the nozzle and antenna ($E_{z\,\max} = E_z|_{r\,=\,0,\,z\,=\,0,h}$), and in the midplane annulus ($E_{r\,\max} = E_r|_{r\,=\,a,\;z\,=\,h/2}$). Studying the field equations, it can be seen that the ratio h/a determines the relative field strengths of those regions. Evaluating the electric field in those regions and applying Eqn. 8[11] to get $J_0(0)$ and $J_1(\chi_{01})$, we find

$$J_n(x) = \frac{1}{\pi}\int_0^{\pi} \cos(n\tau - x\sin\tau)\,d\tau \tag{8}$$

$$\left|\frac{E_z|_{r=0,z=h}}{E_r|_{r=a,z=h/2}}\right| = \left[\frac{\chi_{01}}{\pi}\frac{J_0(0)}{J_1(\chi_{01})}\right]\left(\frac{h}{a}\right) = \left[\frac{2.405}{\pi}\frac{1}{0.52}\right]\left(\frac{h}{a}\right) = 1.472\left(\frac{h}{a}\right) \tag{9}$$

For maximum performance and efficient propellant heating, it is desirable to have the highest concentration of field energy near the nozzle. High field strength in the midplane annulus adversely affects thruster performance. The relative electric field strength in this region is higher when h/a is lower. For this reason, h/a must be properly selected to ensure high relative field strength at the nozzle. To date, METs designed at Penn State have had $h/a \sim 3$.[1]

2.2 Using Eigenfrequency Method to Find Resonance of Modes

In linear algebra, every linear transformation between finite-dimensional vector spaces can be given by a matrix. For many applications, the eigenfrequency f is a more interesting quantity than the eigenvalue λ. They are often related since

$$f = \frac{i\lambda}{2\pi} \tag{10}$$

The eigenvalue solver algorithm leads to the generalized eigenvalue system

$$(\lambda - \lambda_0)^2 EU - (\lambda - \lambda_0)DU + KU + N^T\Lambda = 0 \tag{11}$$

with

$$NU = 0, \tag{12}$$

where the solver evaluates E, D, K, and N for the solution vector U_0 and λ_0 corresponding to the linearization point. The factor λ denotes the eigenvalue. If $E = 0$, it becomes a linear eigenvalue problem, whereas if E is nonzero, it is a quadratic eigenvalue problem. The quadratic eigenvalue problem is solved by reformulating it as a linear eigenvalue problem. After constraint handling, it is possible to write the system in the form $Ax = \lambda Bx$.[12]

3. Numerical Modeling and Discussion of Results

For an empty cavity without any perturbing regions—e.g., dielectric regions or antenna regions—it is fairly straightforward to accurately calculate the cavity's resonant frequency and describe the electric field intensity distribution within the cavity. However, actual METs do contain perturbing regions, which means that analytical solutions are no longer possible to fully characterize the device. Hence, we have employed numerical simulations using

COMSOL Multiphysics to simulate the electric field intensity and distribution within the MET's resonant cavity.

3.1 Simulation Setup

The whole cavity was divided into three different subdomains. The first subdomain is the dielectric cap, which may be defined as Teflon, silica, or quartz with relative permittivities ranging from 2.0 to 4.2. The second subdomain representing the empty portion of the cavity was set to air with permittivity equal to 1. The third subdomain is the coaxial material surrounding the antenna, usually also set to Teflon. Proper boundary conditions must also be set for each model. Three different types of boundary conditions were used in this model. All of the walls and the surface of the antenna were modeled as perfect conductors. The interfaces between different subdomains were modeled as continuous, which ensures that there is a continuous solution through the boundaries. The port was set as coaxial and with 20 W of input power.

The generation of a proper mesh is very important in any numerical solution. The exact number of mesh elements varies depending on the size and shape of the dielectric inserts used; however, the average is around 30,000 elements with approximately 40,000 degrees of freedom. This number of elements was chosen such that an adequate resolution of the problem was acquired, but the computation time was kept to a reasonable level.

3.2 Simulation Result and Discussion

The study of the electric fields focused on three different aspects: the height of the dielectric cap, different dielectric materials for the cap, and the size and shape of the antenna. What we are mostly interested in is the electric field strength near the nozzle and the electric field shape formed within the cavity.

3.2.1 The Eigenfrequency of an Empty Cavity

The purpose of solving for the eigenfrequency is to quickly find the resonant frequency at any given mode of interest. Fig. 4(a) and Fig. 4(b) show the electric field intensity and electric field streamlines of the TM^{z}_{011} mode, whereas Fig. 4(c) and Fig. 4(d) show other modes that are not useful in the MET. Again, for an empty cavity, it is easy to determine the resonant frequency. However, for the cavity loaded with dielectric and with a probe inserted, the prediction becomes very inaccurate. Accurate determination of the resonant frequency requires small frequency steps over a large frequency range. Hence, using the eigenfrequency method saves significant solution time. It is should be noted that the eigenfrequency does not equal the resonant frequency, because the eigenfrequency is where cavity absorbs the most energy, but what we want is largest electric field near the nozzle.

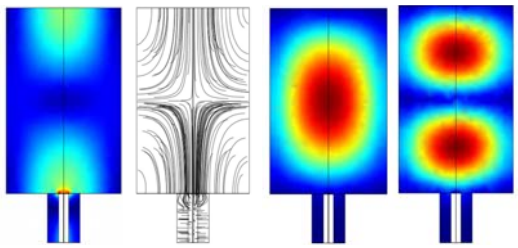

(a) (b) (c) (d)

Figure 4. Distribution of electric intensity; (b) electric streamlines; (c),(d) useless modes

3.2.2 Cavity with Increasing Cap Height

As discussed in Section 2, plasma formation near the antenna causes antenna erosion, which is undesirable. In previous MET instantiations, the method used to keep plasma from forming near the antenna was to placing a piece of quartz (permittivity of 4.2) at the midplane of the cylindrical cavity. For lower frequency METs, (i.e., 2.45 GHz and 7.5 GHz) the midplane plate works very well, but the cavity discussed in this paper is much smaller (only 8.33 mm in diameter and 27 mm in height), so a dielectric cap covering the antenna was investigated.

In order to test the geometry size effect of the cap, cap diameter was kept as same as the cavity while cap height changed at 3 mm, 6 mm and 9 mm. Teflon with permittivity 2.0 was used as the cap material. As shown in Fig. 5, when the height increases, both the resonant frequency and electric field strength drops. The electric field strengths for the empty cavity, 3-mm, 6-mm, and 9-mm cap height are shown in

Fig. 6(a)–(d). Although two strong peaks are shown in Fig. 5, only the one at 14.535 GHz is the TM^{z}_{011} mode. It is also necessary to explain why the electric field strength of cavity with cap is larger than that of an empty cavity. In an empty cavity, the electric field is symmetric with respect to the midplane of the cavity and, accordingly, the power absorbed by the cavity is divided into two parts, whereas the cap makes the cavity asymmetric, so the power increases on one side of cavity and decreases on the other side.

3.2.3 Cavity with Different Cap Material

Here we keep the cap shape the same and change the cap material. Teflon, silica, and boron nitride were the three different materials investigated, with dielectric permittivities of 2.0, 3.0 and 4.2, respectively. It is evident from Fig.7 that increasing the dielectric permittivity of the material causes a decrease in the resonant frequency and electric field strength in the cavity. Fig. 8(a)–(c) shows the electric fields using Teflon, silica, and quartz.

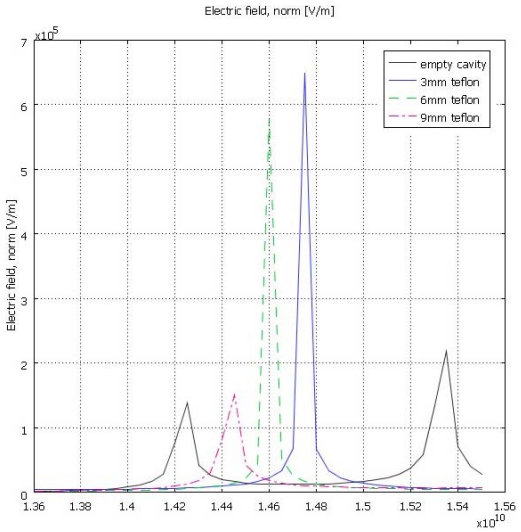

Figure 5. Electric field strength change with different cap height

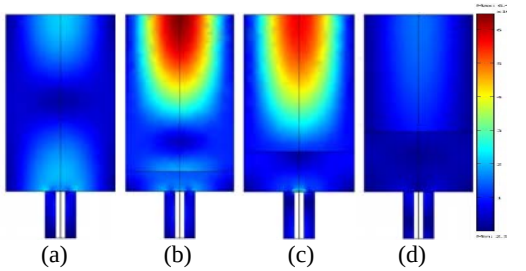

Figure 6. (a) Magnitude and distribution of electric field intensity in an empty cavity; (b) 3-mm cap; (c) 6-mm cap; (d) 9-mm cap

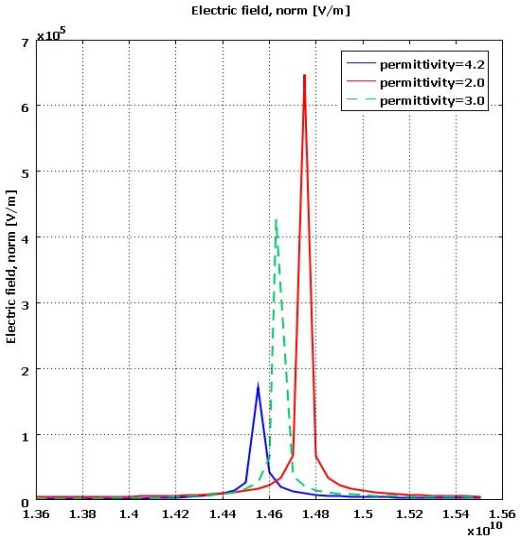

Figure 7. Electric field strength changes with different cap material.

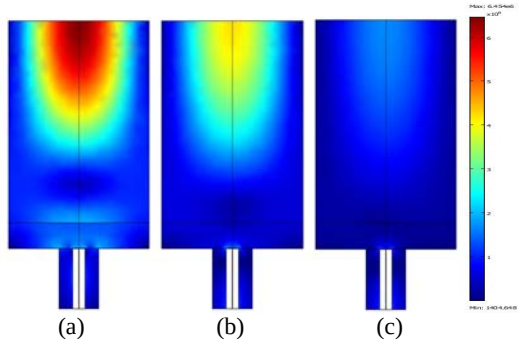

Figure 8. Magnitude and distribution of electric intensity with permittivity (a) 2.0; (b) 3.0; (c) 4.2.

3.2.4 Antenna Shape Effects

The MET was also modeled with different antenna protrusion depths and shapes. The protrusion depth is the amount that the inner conductor of the input coaxial cable protrudes

into the resonant cavity. Two different antenna shapes were also modeled: one was a cylindrical flat-topped antenna and the other was a cylindrical antenna with its end rounded, such that there were no sharp edges.

The tested antenna depths were 0 mm, 1 mm, and 1.6985 mm (with round tip) and 2 mm. Fig.9 shows that, with respect to the antenna depth, as antenna depth increases, the field strength drops (see Fig. 10(a)–(d) for field distributions). However, the bandwidth of resonance became wider. That is to say, although we sacrifice some field strength, we get larger frequency range over which the cavity is resonant, which makes the cavity less sensitive to the plasma. Rounding the antenna tip equates to a decrease in its depth. It was also found that the resonant frequency dropped as the protrusion depth increased.

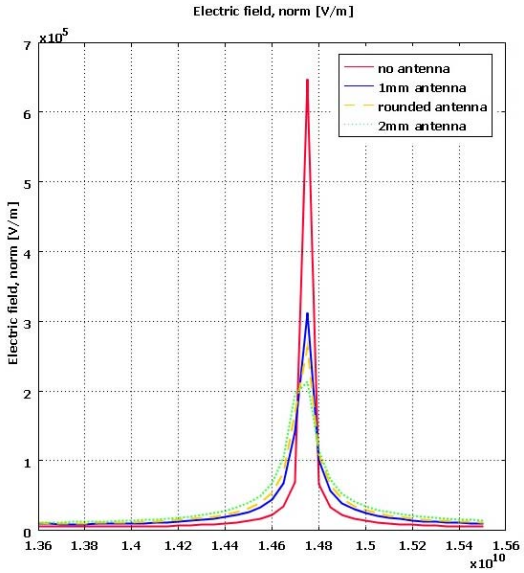

Figure 9. Electric field strength change with different antenna depth and shape.

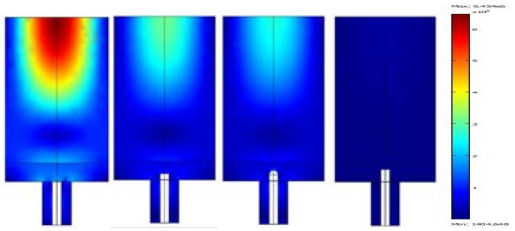

Figure 10. Magnitude and distribution of electric intensity (a) no antenna protrusion; (b) antenna depth 1 mm; (c) antenna depth 1.6985 mm and rounded; (d) antenna depth 2 mm.

4. Conclusions and Future work

The overall goal of this modeling effort is to model the physical processes behind the operation of a 20-W, 14.5-GHz MET. The analytical solutions to Maxwell's Equations were derived for the empty MET resonant cavity. A solution that predicts the resonant frequency of a dielectric-loaded cavity was also derived. COMSOL Multiphysics was used to perform numerical electromagnetic modeling of the electric field in the resonant cavity of the cavity. Parametric studies were performed to determine effects of finding the TM^{z}_{011} mode with eigenfrequency, varying dielectric materials inside the cavity, and varying antenna depth.

Results of these simulations show that inserting a dielectric cap into the cavity significantly alters the electric-field structure and lowers the resonant frequency as well. For increasing cap height, the resonant frequency and electric field strength decrease. Similarly, increasing the permittivity of dielectric material caused a decrease in the resonant frequency and electric field strength. Numerical modeling also provided insight on the effects of varying antenna depth and tip shape. In general, a decrease in resonant frequency and maximum electric field strength, and an increase in resonant bandwidth, were observed with increasing antenna depth. Rounding an antenna at a given depth equates to decreasing its protrusion depth.

The ultimate goal of this work is to create a full multiphyiscs model of the MET. This model will combine together electromagnetic modeling, plasma physics (i.e., gas breakdown), fluid flow, and thermal dynamics. COMSOL Multiphysics is an excellent choice for developing this multiphysics model.

5. References

1. Clemens, D.E., "Performance Evaluation of the Microwave Electrothermal Thruster Using Nitrogen, Simulated Hydrazine, and Ammonia," Doctor of Philosophy Thesis, Department of Aerospace Engineering, The Pennsylvania State University (2008).

2. Bilén, S.G., C.J. Valentino, M.M. Micci, and D.E. Clemens, "Numerical Electromagnetic

Modeling of a Low-Power Microwave Electrothermal Thruster," *AIAA Paper 2005-3699* (2005).
3. Frasch, L.L., J.M. Griffin, and J. Asmussen, "An Analysis of Electromagnetic Coupling and Eigenfrequencies for Microwave Electrothermal Thruster Discharges," *AIAA Paper 1984–1521* (1984).
4. Frasch, L., and J. Asmussen, "Electromagnetic Plasma Models for Microwave Plasma Reactors," *AIAA Paper 1984–1521* (1984).
5. Power, J.L., "Microwave Electrothermal Propulsion for Space," *IEEE Trans. Microwave Theory and Techniques*, **Vol. 40**, **No. 6**, pp. 1179–1191 (1992).
6. Micci, M.M., and P. Balaam, "Investigation of Free-Floating Resonant Cavity Microwave Plasma for Propulsion," *Journal of Propulsion and Power*, **Vol. 8**, **No. 1**, pp. 103–109 (1992).
7. Balaam, P., and M.M. Micci, "Investigation of Stabilized Resonant Cavity Microwave Plasma for Propulsion," *Journal of Propulsion and Power*, **Vol. 11**, **No. 5**, pp. 1021–1027 (1995).
8. Souliez, F.J., S.G. Chianese, G.H. Dizac, and M.M. Micci, "Low-Power Microwave Arcjet Testing: Plasma and Plume Diagnostic and Performance Evaluation," *Micropropulsion for Small Spacecraft*, edited by M.M. Micci and A.D. Ketsdever, **Vol. 187**, Progress in Astronautics and Aeronautics, AIAA, Reston, VA, pp. 199–214 (2000).
9. Juan, Y., H. Hongqing, M. Genwang, and H. Xianwei, "Resonant and Ground Experimental Study on Microwave Plasma Thruster," *J. Spacecraft and Rockets*, **Vol. 41**, **No. 1**, pp. 126–131 (2004).
10. Pozar, D.M., *Microwave Engineering, 3rd ed.*, Addison-Wesley Publishing Company, Inc., New York (2005).
11. Abramowitz, M., and I.A. Stegun, *Handbook of Mathematical Functions with Formulas, Graphs, and Mathematical Tables*, ninth Dover printing, tenth GPO printing, New York (1964).
12. COMSOL AB, *COMSOL Multiphysics User's Guide,* Version 3.3, (August 2006).